

Enhancement of the Catalytic Activity of a Macrocyclic Cobalt(II) Complex for the Electroreduction of O₂ by Adsorption on Graphite

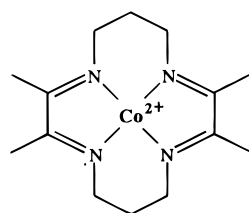
Iqbal Bhugun and Fred C. Anson*

Arthur Amos Noyes Laboratories, Division of Chemistry and Chemical Engineering,
California Institute of Technology, Pasadena, California 91125

Received July 17, 1996[⊗]

In solution, the [(tim)Co]²⁺ complex (tim = 2,3,9,10-tetramethyl-1,4,8,11-tetraazacyclotetradeca-1,3,8,10-tetraene) reacts only slowly with O₂, but upon adsorption on graphite electrodes, it becomes an active catalyst for the reduction of O₂ to H₂O₂. The electroreduction of O₂ proceeds in a single voltammetric step at close to the diffusion-controlled rate at a relatively positive potential (0.25 V vs SCE). The remarkable enhancement in catalytic activity is attributed to a higher affinity for O₂ of the adsorbed complex as a result of its interactions with functional groups on the surface of roughened or oxidized graphite. A possible mechanism for the catalytic reduction of O₂ is proposed. It differs from the one employed by the analogous [(hmc)Co]²⁺ complex (hmc = *C-meso*-5,7,7,12,14,14-hexamethyl-1,4,8,11-tetraazacyclotetradecane) which operates at less positive potentials and exhibits two separated voltammetric steps in the reduction of O₂, via [(hmc)CoOOH]²⁺, to H₂O₂.

With the objective of learning more about the details of the mechanisms through which complexes of Co(II) with macrocyclic ligands (including porphyrins) catalyze the electroreduction of O₂, we have hopefully studied the electrochemical behavior of several macrocyclic complexes of Co(II) in the presence of O₂.^{1–6} Among the appealing features of these water-soluble catalysts for the electroreduction of O₂ are the opportunities they afford to observe the electrochemical behavior of some of the intermediates that are formed during the catalytic cycles. In addition, the coordination chemistry and redox reactivity exhibited by these complexes in homogeneous solutions containing O₂ have been extensively documented in previous reports by Endicott and co-workers^{7–9} and Espenson and co-workers.^{10–15} We were attracted to the [(tim)Co]²⁺



[(tim)Co]²⁺

complex (tim = 2,3,9,10-tetramethyl-1,4,8,11-tetraazacyclotet-

radeca-1,3,8,10-tetraene) by the recent reports of Marchaj et al.^{13,14} that the complex participates in redox reactions that accomplish the direct, four-electron reduction of O₂ to H₂O without passing through H₂O₂ as an intermediate. Since the same process at electrodes is difficult to achieve and is the object of current work in many groups, we decided to examine the electrochemistry of [(tim)Co]²⁺ in the presence and absence of O₂. The results, described in this report, showed the complex to be catalytically inactive toward O₂ when generated by electroreduction of [(tim)Co]³⁺ in solution. However, when adsorbed on the surface of roughened graphite electrodes, the catalytic activity of the complex was so greatly enhanced that the electroreduction of O₂ (to H₂O₂) became diffusion-controlled.

Experimental Section

Reagent quality chemicals were used as received from commercial sources. Laboratory distilled water was further purified by passage through a purification train (Milli-Q Plus, Millipore Co.). [(tim)Co-(H₂O)₂] (CF₃SO₃)₂ was prepared by the literature procedure.¹³ UV-vis spectra in aqueous solution: ε₅₄₄ = 3400 M⁻¹ cm⁻¹; the reported value is 3450 M⁻¹ cm⁻¹.¹³ Anal. Calcd for C₁₆H₂₈N₄O₈F₆Co: C, 29.96; H, 4.40; N, 8.73. Found: C, 29.80; H, 4.57; N, 8.75. The complex was stored in a refrigerator at ca. 4 °C. [(tim)Co]³⁺ was prepared in solution by electrolytic oxidation of [(tim)Co]²⁺ at a reticulated glassy carbon electrode of high surface area (~200 cm²) under argon in a three-compartment cell.

Apparatus and Procedures. Electrochemical measurements were performed with conventional commercially available instrumentation and two- or three-compartment cells with the compartments separated by fine-porosity glass frits. The counter electrode was a platinum coil (20 cm²). Reference electrodes were either a standard saturated calomel electrode (SCE) or a sodium chloride-saturated calomel electrode. All potentials are quoted with respect to the SCE. The graphite working electrodes for rotating disk and cyclic voltammetric experiments were constructed by using heat-shrinkable polyolefin tubing to attach edge plane pyrolytic graphite (EPG) rods (Union Carbide Co.) to stainless shafts adapted to fit the rotator. The Pt ring-pyrolytic graphite disk electrode (Pine Instruments Co., Model AFMT28T) had a collection efficiency of 27%. The platinum ring was pretreated electrochemically by cycling between +1.3 and -0.2 V in 0.5 M sulfuric acid until well-defined hydrogen adsorption peaks were obtained. Rotating disk voltammetry was carried out with a scan rate of 5 mV s⁻¹.

Highly polished EPG electrodes were prepared by polishing with 0.3 μm alumina (Buehler Co.) on a polishing cloth to obtain a mirrorlike

* Corresponding author.

[⊗] Abstract published in *Advance ACS Abstracts*, November 15, 1996.

- (1) Geiger, T.; Anson, F. C. *J. Am. Chem. Soc.* **1981**, *103*, 7489.
- (2) Bowers, M. L.; Anson, F. C. *J. Electroanal. Chem.* **1984**, *171*, 269.
- (3) Durand, R. R.; Webley, S. W.; Anson, F. C. *J. Electroanal. Chem.* **1987**, *229*, 273.
- (4) Quyang, O.; Anson, F. C. *J. Electroanal. Chem.* **1989**, *271*, 331.
- (5) Kang, C.; Anson, F. C. *Inorg. Chem.* **1995**, *34*, 2771.
- (6) Kang, C.; Xie, Y.; Anson, F. C. *J. Electroanal. Chem.*, in press.
- (7) Wong, C.-L.; Switzer, J. A.; Balakrishnan, B. P.; Endicott, J. F. *J. Am. Chem. Soc.* **1980**, *102*, 5511.
- (8) Wong, C.-L.; Endicott, J. F. *Inorg. Chem.* **1981**, *20*, 2233.
- (9) Kumar, K.; Endicott, J. F. *Inorg. Chem.* **1984**, *23*, 2447.
- (10) Bakac, A.; Espenson, J. H. *Inorg. Chem.* **1990**, *29*, 2062.
- (11) Bakac, A.; Espenson, J. H. *J. Am. Chem. Soc.* **1990**, *112*, 2273.
- (12) Marchaj, A.; Bakac, A.; Espenson, J. H. *Inorg. Chem.* **1992**, *31*, 4164.
- (13) Marchaj, A.; Bakac, A.; Espenson, J. H. *Inorg. Chem.* **1992**, *31*, 4860.
- (14) Marchaj, A.; Bakac, A.; Espenson, J. H. *Inorg. Chem.* **1993**, *32*, 2399.
- (15) Wang, W.-D.; Bakac, A.; Espenson, J. H. *Inorg. Chem.* **1995**, *34*, 4049.

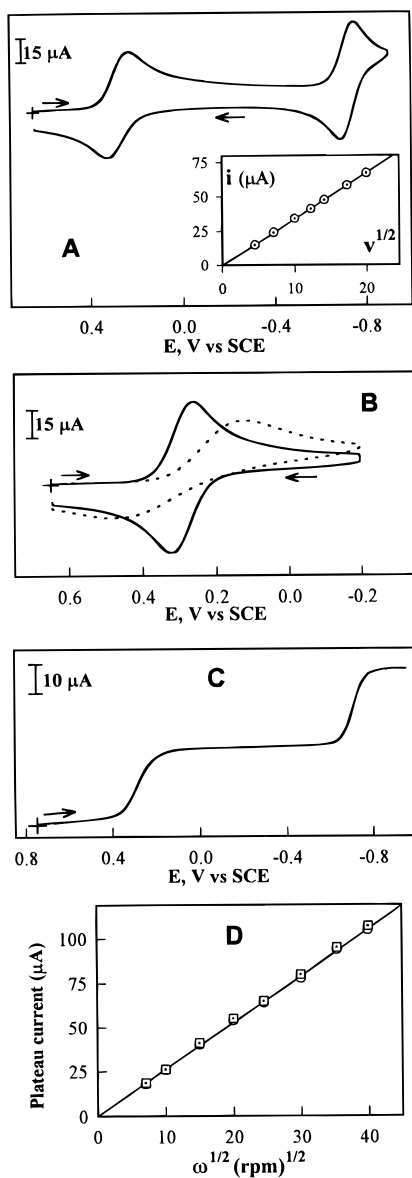


Figure 1. Voltammetry of $[(\text{tim})\text{Co}]^{3+}$. (A) Cyclic voltammogram for 1.25 mM $[(\text{tim})\text{Co}]^{3+}$ recorded at 100 mV s^{-1} with a freshly polished EPG electrode (0.2 cm^2). Supporting electrolyte: 0.2 M CF_3COONa . The inset gives the dependence of the first cathodic peak current on (scan rate) $^{1/2}$ ($\text{mV s}^{-1/2}$). (B) Repeat of part A with a glassy carbon electrode which had not been freshly polished (dotted curve) or with a freshly polished EPG electrode from which residual alumina particles had not been removed by sonication (solid curve). (C) Current-potential curve for the reduction of 1.25 mM $[(\text{tim})\text{Co}]^{3+}$ at a polished rotating EPG disk electrode. Rotation rate: 100 rpm. Supporting electrolyte: 0.2 M CF_3COONa . (D) Levich plots of the two plateau currents in part C: (O) first plateau; (□) second plateau.

surface followed by a second polishing step (1–3 min) on a separate cloth with abundant water but no alumina. To obtain roughened EPG electrodes the polishing was carried out with 600 grit SiC paper (3M Co.). After either polishing procedure the electrodes were sonicated in pure water for several minutes. Levich currents for the reduction of O_2 were calculated by using the following parameters: kinematic viscosity of water, $0.01 \text{ cm}^2 \text{ s}^{-1}$; concentration of dioxygen- and air-saturated solutions, 1.38 and 0.28 mM, respectively; diffusion coefficient of O_2 , $1.8 \times 10^{-5} \text{ cm}^2 \text{ s}^{-1}$. Experiments were conducted at the ambient laboratory temperature $22 \pm 2 \text{ }^\circ\text{C}$.

Results

Electrochemistry of $[(\text{tim})\text{Co}]^{3+}$ in the Absence of O_2 . Shown in Figure 1 are cyclic and rotating disk voltammograms

for $[(\text{tim})\text{Co}]^{3+}$ recorded at a highly polished EPG electrode in the absence of O_2 . The two reversible voltammetric responses in Figure 1A correspond to the $[(\text{tim})\text{Co}]^{3+/2+}$ and $[(\text{tim})\text{Co}]^{2+/+}$ couples with formal potentials, +0.29 and -0.70 V , that match the previously reported values. 16,17 The smaller peak currents and larger peak separations obtained for the $[(\text{tim})\text{Co}]^{3+/2+}$ than for the $[(\text{tim})\text{Co}]^{2+/+}$ couple reflect the smaller heterogeneous electron-transfer rate constant for the former couple. The estimated rate constant for electron self-exchange for the $[(\text{tim})\text{Co}]^{3+/2+}$ couple is $k_{\text{ex}} = 5 \times 10^{-2} \text{ M}^{-1} \text{ s}^{-1}$. 17 Using the Marcus relation, $k_{\text{het}} \approx (10^{-3}k_{\text{ex}})^{1/2}$, 18,19 the corresponding heterogeneous rate constant can be estimated as $k_{\text{het}} = 7 \times 10^{-3} \text{ cm s}^{-1}$. However, the Marcus relation depends on the assumption that the electron-transfer follows outer-sphere pathways both in solution and at the electrode surface. In fact, the electrochemical response exhibited a high sensitivity to the type and pretreatment of the electrode (Figure 1B) so that an inner-sphere pathway is indicated for the heterogeneous electron transfer.

In contrast to the cyclic voltammetric peak currents, the two cathodic plateau currents obtained at a rotated disk electrode were of equal magnitude (Figure 1C) and both increased linearly with the electrode (rotation rate) $^{1/2}$ (Figure 1D). The diffusion coefficient for $[(\text{tim})\text{Co}]^{3+}$ calculated from the slope of the two coincident lines in Figure 1D was $3.8 \times 10^{-6} \text{ cm}^2 \text{ s}^{-1}$, which matches the value measured recently for a related macrocyclic complex of Co(II) of essentially the same size. 5

On the basis of the results shown in Figure 1, one may regard the $[(\text{tim})\text{Co}]^{3+/2+}$ couple as reasonably well-behaved at polished EPG electrodes with an electron-transfer rate constant large enough to sustain significant currents for catalytic cycles involving the $[(\text{tim})\text{Co}]^{3+/2+}$ couple.

Electrochemistry of $[(\text{tim})\text{Co}]^{3+}$ in the Presence of O_2 .

Espenson and co-workers reported that in dioxygen-saturated solutions the $[(\text{tim})\text{Co}]^{2+}$ complex is oxidized at a very low rate with a pseudo-first-order rate constant of $5 \times 10^{-6} \text{ s}^{-1}$. 13 This reaction rate is much too low for the presence of O_2 to affect the cyclic voltammetry of the $[(\text{tim})\text{Co}]^{3+/2+}$ couple at typical scan rates, and as expected, the reversible voltammetric response near 0.3 V is unchanged by the addition of O_2 (compare the solid and dashed curves in Figure 2A). However, there is a second, broad cathodic peak near -0.2 V in the presence of O_2 (solid curve in Figure 2A) that does not arise from the direct reduction of O_2 at the electrode because it is not present in solutions containing no $[(\text{tim})\text{Co}]^{3+}$ (dotted curve in Figure 2A). The cathodic peak near -0.20 V might be ascribed to the reduction of an O_2 adduct, $[(\text{tim})\text{CoOO}]^{2+}$, formed by the reaction of O_2 with $[(\text{tim})\text{Co}]^{2+}$ generated in the diffusion-convection layer at the surface of the rotated electrode. Electrochemical reduction of such adducts have been described in previous studies of the $[(\text{cyclam})\text{Co}]^{3+/2+}$ (cyclam = 1,4,8,11-tetraazacyclotetradecane) 1 and $[(\text{hmc})\text{Co}]^{3+/2+}$ (hmc = *C-meso*-5,7,12,14,14-hexamethyl-1,4,8,11-tetraazacyclotetradecane) 5 complexes in the presence of O_2 , although, in these cases, the reductions of the Co^{3+} complexes and their strongly oxidizing O_2 adducts were superimposed instead of occurring in separated steps as in Figure 2A. The equilibrium constant for the formation of $[(\text{tim})\text{CoOO}]^{2+}$ from $[(\text{tim})\text{Co}]^{2+}$ and O_2 has been estimated as $\sim 1 \text{ M}^{-1}$ 14 so that very little of the adduct is present in solutions of $[(\text{tim})\text{Co}]^{2+}$ that are saturated with O_2 ($[\text{O}_2] =$

(16) Rillema, D. P.; Endicott, J. F. *Inorg. Chem.* **1976**, *15*, 1459.

(17) Endicott, J. F.; Durham, B.; Glick, M. D.; Anderson, T. J.; Kuszaj, J. M.; Schmonsees, W. G.; Balakrishnan, K. P. *J. Am. Chem. Soc.* **1981**, *103*, 1431.

(18) Marcus R. A. *Electrochim. Acta* **1968**, *13*, 995.

(19) Bard, A., Faulkner, L. R. *Electrochemical Methods*; John Wiley and Sons: New York, 1980; p 620.

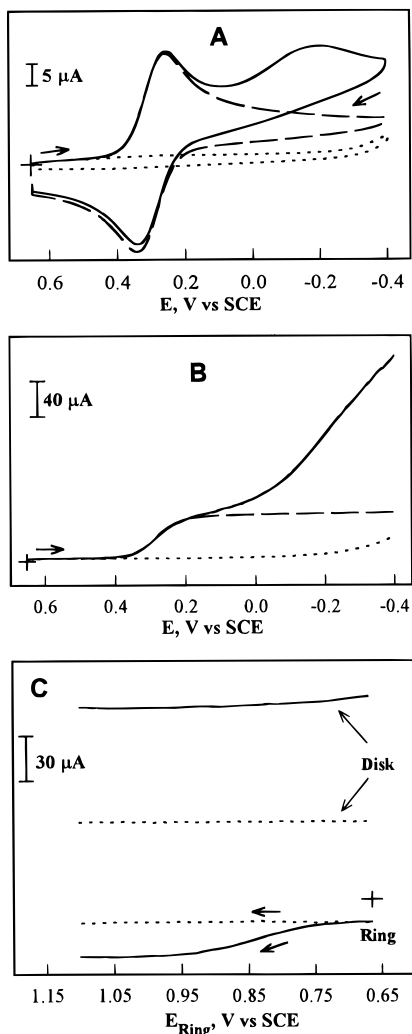


Figure 2. (A) Cyclic voltammetry at a highly polished EPG electrode (0.2 cm^2) for $1.1 \text{ mM } [(tim)Co]^{3+}$ in the absence of O_2 (dashed curve) and in an air-saturated solution (solid curve). Scan rate: 50 mV s^{-1} . The dotted curve was obtained with the air-saturated solution in the absence of $[(tim)Co]^{3+}$. Supporting electrolyte: $0.2 \text{ M CF}_3\text{COONa}-0.2 \text{ M CF}_3\text{COOH}$. (B) Current-potential curves at a highly polished rotating EPG disk electrode (0.17 cm^2) for the reduction of $1.3 \text{ mM } [(tim)Co]^{3+}$ in the absence of O_2 (dashed curve) and for the reduction of O_2 in the absence and presence of $[(tim)Co]^{3+}$. Key: solid curve, $1.3 \text{ mM } [(tim)Co]^{3+}$ in a solution saturated with O_2 ; dotted curve, reduction of O_2 in the absence of $[(tim)Co]^{3+}$. Supporting electrolyte as in part A. Electrode rotation rate: 600 rpm . (C) Current-potential responses for $1.3 \text{ mM } [(tim)Co]^{3+}$ at the rotating ring-disk electrode in the absence and presence of O_2 . Dotted lines: reduction of $[(tim)Co]^{3+}$ at the disk and oxidation of $[(tim)Co]^{2+}$ at the ring electrode in the absence of O_2 . The disk potential was maintained at -0.2 V . The ring current was recorded as the potential of the ring electrode was scanned from 0.65 to 1.10 V at 5 mV s^{-1} . Solid curves: The corresponding responses after the solution was saturated with O_2 . Other conditions were as in part B. The + sign marks the point of zero current for both electrodes.

1.38 mM). However, reduction currents as large as those at the second cathodic peak in Figure 2A would be possible if the rate of formation of the O_2 adduct were sufficiently high and its electroreduction regenerated $[(tim)Co]^{2+}$ so that a catalytic reduction of O_2 ensued.

The reductions of $[(tim)Co]^{3+}$ at a rotating disk electrode in the presence and in the absence of O_2 and of O_2 in the absence of $[(tim)Co]^{3+}$, are shown in Figure 2B. The $[(tim)Co]^{2+}$ generated at the surface of the disk electrode clearly causes the electroreduction of O_2 to commence at potentials ($\sim 0.1 \text{ V}$) where it is not reduced in solutions containing no $[(tim)Co]^{3+}$

(dotted curve in Figure 2B). The course of the catalytic reaction was monitored by using a rotating ring-disk electrode²⁰ to determine the products of the cathodic reactions at the disk electrode by oxidizing them at the ring electrode as shown in Figure 2C. The dotted lines are the disk and ring currents measured in the absence of O_2 with the disk potential maintained at -0.2 V (where $[(tim)Co]^{3+}$ was reduced to $[(tim)Co]^{2+}$) while the potential of the ring electrode was scanned from 0.65 to 1.10 V . Throughout this potential range $[(tim)Co]^{2+}$ generated at the disk electrode was oxidized to $[(tim)Co]^{3+}$ at the ring so that both the disk and ring currents remained constant. The solid curves resulted after the solution was saturated with O_2 . The disk current increased because of the catalytic reduction of O_2 at the disk potential of -0.2 V . The presence of O_2 had no effect on the anodic ring current at ring potentials less positive than 0.70 V because the product of the reduction of O_2 at the disk (H_2O or H_2O_2) is not oxidizable at these potentials. The increase in ring current near 0.8 V leading to a current plateau at 1.0 V demonstrated that a product of the catalytic reduction of O_2 at the disk was oxidizable at the ring at these potentials, a property consistent with H_2O_2 but not H_2O . The ratio of the increased ring and disk currents in the presence of O_2 corresponded to the known collection efficiency²⁰ of the ring-disk electrode, showing that the catalyzed reduction of O_2 produced only H_2O_2 .

To determine if the mechanism of the catalytic reduction of O_2 involved an O_2 adduct, $[(tim)CoOO]^{2+}$, formed in solution, cyclic voltammograms were recorded in solutions saturated with O_2 and containing different concentrations of $[(tim)Co]^{3+}$. The results are shown in Figure 3A. At concentrations of $[(tim)Co]^{3+}$ greater than ca. 0.3 mM the magnitude of the second peak in the voltammograms, which results from the catalyzed reduction of O_2 , becomes almost independent of the concentration of $[(tim)Co]^{3+}$. Indeed, when the contributions to the currents from the continuing reduction of $[(tim)Co]^{3+}$ are subtracted, the second cathodic peak currents are essentially constant (Figure 3B). Only when the concentration of $[(tim)Co]^{3+}$ was decreased below ca. 0.3 mM did the peak current for the reduction of O_2 begin to diminish (Figure 3B).

Catalytic reduction currents that become independent of the concentration of catalyst in the presence of excess substrate (O_2) are not compatible with a catalytic mechanism in which a catalyst-substrate adduct formed in solution, $[(tim)CoOO]^{2+}$, is reduced at the second cathodic peak. A different mechanism for the catalytic reduction is required. An alternative mechanism that is compatible with the insensitivity of the catalytic current to the concentration of catalyst is one in which only catalyst molecules adsorbed on the electrode surface participate. Once the surface is saturated with the active, adsorbed catalyst, further increases in its concentration in solution could not affect the catalytic current. Although the cyclic voltammetry of the $[(tim)Co]^{3+/2+}$ couple showed no evidence of adsorption at highly polished EPG electrodes (inset in Figure 1A), the quantity of adsorbed catalyst necessary to produce the second cathodic peak in Figure 2A could be too small to perturb the linearity of the plots of peak current vs (scan rate)^{1/2} in the absence of O_2 . Electrodes that were exposed to solutions of $[(tim)Co]^{3+}$ for a few minutes and then transferred to pure supporting electrolyte solutions to search for evidence of any irreversibly adsorbed complex showed none. However, when the same experiment was repeated with O_2 present in the pure supporting electrolyte, evidence for the transient presence of an adsorbed catalyst on the electrode surface was found in the form of catalytic reduction

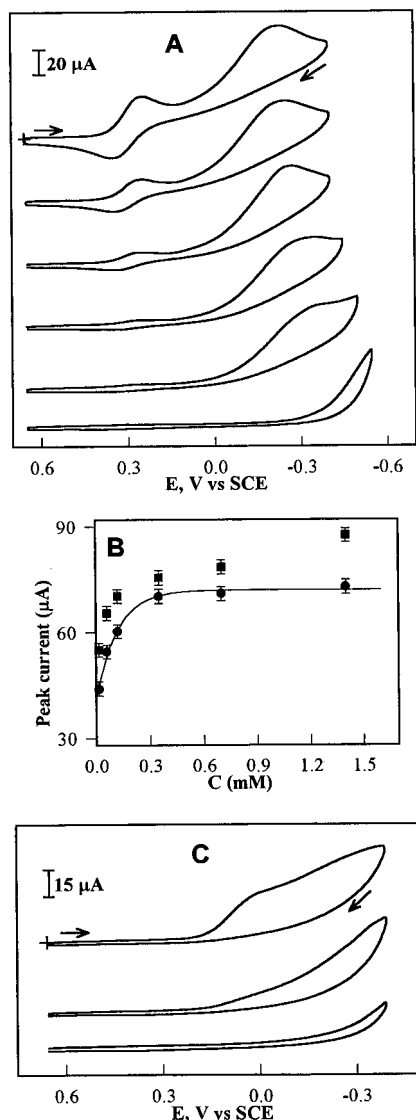


Figure 3. Effect of the concentration of $[(\text{tim})\text{Co}]^{3+}$, C , on cyclic voltammograms for the catalytic reduction of O_2 . (A) Concentrations of $[(\text{tim})\text{Co}]^{3+}$ were, from top to bottom: 1.35, 0.67, 0.35, 0.12, 0.06, 0 mM. Scan rate: 50 mV s^{-1} . Supporting electrolyte: 0.2 M CF_3COONa –0.2 M CF_3COOH saturated with O_2 . (B) Peak currents of the second cathodic waves in part A vs the concentration of $[(\text{tim})\text{Co}]^{3+}$: (■) Peak currents measured with respect to the baseline in the pure supporting electrolyte saturated with argon; (●) peak currents measured with respect to the current in the same solution of $[(\text{tim})\text{Co}]^{3+}$ in the absence of O_2 . (C) Cyclic voltammograms recorded with a freshly polished electrode that was dipped in 1.3 mM $[(\text{tim})\text{Co}]^{3+}$ for 15 min, washed, and transferred to 0.2 M CF_3COONa –0.2 M CF_3COOH saturated with O_2 . Key: top curve, first scan; middle curve, second scan; bottom curve, first scan after the electrode was dipped for 15 min in a solution containing no $[(\text{tim})\text{Co}]^{3+}$. Scan rate: 50 mV s^{-1} .

currents that declined steadily, presumably because the catalyst gradually desorbed from the electrode surface (Figure 3C).

Another experimental feature pointing to the adsorbed $[(\text{tim})\text{Co}]^{2+}$ complex as the site of the catalytic reduction of O_2 was the difference in the reproducibility of the voltammetric response for the $[(\text{tim})\text{Co}]^{3+/2+}$ couple and that for the catalytic reduction of O_2 . On freshly polished electrodes, the response from the reversible $[(\text{tim})\text{Co}]^{3+/2+}$ couple was reproducible and stable under continuous cycling of the electrode potential. In contrast, the current–potential curves for the reduction of O_2 were highly dependent on the pretreatment of the electrode surface. Careful polishing, sonication, and precycling of the electrode in pure supporting electrolyte over the potential range of interest were

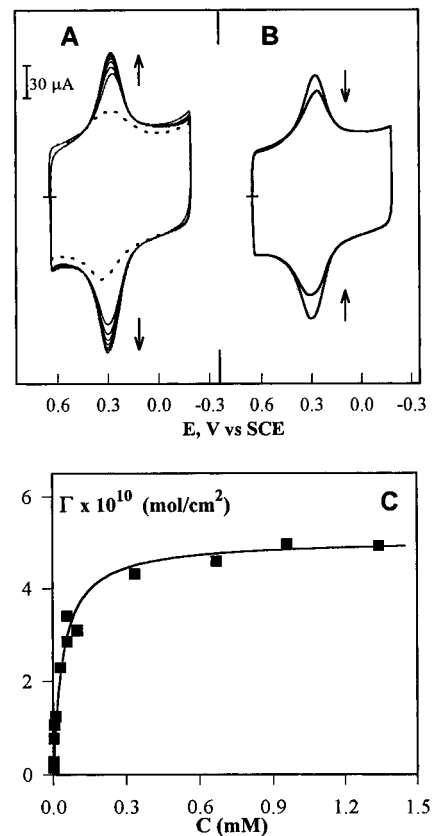


Figure 4. Cyclic voltammetry of $[(\text{tim})\text{Co}]^{3+}$ at a roughly polished EPG electrode (0.32 cm^2). (A) Voltammograms recorded continuously at 300 mV s^{-1} after the roughly polished electrode was placed in a 0.12 mM solution of $[(\text{tim})\text{Co}]^{3+}$. The dotted curve is the response obtained in the absence of $[(\text{tim})\text{Co}]^{3+}$ from reduction and oxidation of functional groups (quinone, etc.) on the freshly roughened electrode. (B) Cyclic voltammetry after the electrode used to record the increasing peak currents in part A was transferred to pure supporting electrolyte (0.2 M CF_3COONa –0.2 M CF_3COOH). The two curves were recorded immediately after transfer and 30 s later. (C) Quantity of $[(\text{tim})\text{Co}]^{3+}$ adsorbed on roughly polished EPG electrodes from solutions containing various concentrations of the complex.

required to obtain reproducible responses for the catalytic reduction of O_2 near -0.2 V . The behavior indicated that careful pretreatment of electrode surfaces was required to reproduce the extent of adsorption of the $[(\text{tim})\text{Co}]^{2+}$ catalyst and the corresponding catalytic currents from run to run.

Electrochemistry of $[(\text{tim})\text{Co}]^{3+}$ at Roughened EPG Electrodes. It was possible to enhance the adsorption of the $[(\text{tim})\text{Co}]^{3+/2+}$ couple on EPG electrodes by creating a rougher surface than resulted from polishing with $0.3 \mu\text{m}$ alumina particles. The desired roughness was obtained by using polishing paper coated with $15.3 \mu\text{m}$ particles of SiC. The cyclic voltammograms in Figure 4A were recorded in a dilute solution of $[(\text{tim})\text{Co}]^{3+}$ with an electrode polished with the SiC paper. The peak currents increased with time as expected if the complex gradually accumulated on the rougher electrode surface. The more symmetrical shape of the voltammograms compared with those in Figure 1A is also indicative of a response that is dominated by an adsorbed reactant. The $[(\text{tim})\text{Co}]^{3+}$ adsorbed on the surface of the roughened EPG electrode used to record the voltammograms in Figure 4A remained on the surface temporarily when the electrode was transferred to a pure supporting electrolyte solution as shown in Figure 4B. However, the complex gradually desorbed into the solution as indicated by the decay in the peak current.

The quantity of $[(\text{tim})\text{Co}]^{3+}$ adsorbed on roughened EPG electrodes was measured by numerically integrating the area

encompassed by the cathodic peaks in cyclic voltammograms like those in Figure 4A between potentials on either side of the reduction peak (0.65–0 V) and subtracting the area calculated for the response of the [(tim)Co]³⁺ in solution and the contribution to the area from surface functional groups (dotted curve in Figure 4A). The results are shown in Figure 4C. The adsorption attains a limiting value of ca. 5×10^{-10} mol cm⁻² (geometric area) and it reaches half-saturation at a concentration of [(tim)Co]³⁺ of ca. 0.05 mM. Attempts to apply the same procedure to highly polished EPG electrodes produced only an upper limit on the adsorption of $\sim 2 \times 10^{-11}$ mol cm⁻². The much more extensive adsorption on the roughened EPG surface is attributed both to a larger microscopic electrode area and the availability of more functional groups (carbonyl, carboxylate, etc.) for possible axial coordination to the Co center of the adsorbed complex.

Catalysis of the Reduction of O₂ by Adsorbed [(tim)Co]^{3+/2+} on Roughened EPG Electrodes. In Figure 5A are shown cyclic voltammograms for a 0.1 mM solution of [(tim)Co]³⁺ at a roughened EPG electrode in the absence (dotted curve) and in the presence (solid line) of O₂. The response in the presence of O₂ is remarkably different from that obtained at the highly polished EPG electrode in Figure 2A. The catalysis of the reduction of O₂ begins at the potential where [(tim)Co]³⁺ is reduced to [(tim)Co]²⁺ instead of at more negative potentials and the catalytic peak current is larger. The enhanced catalytic activity must arise entirely from the adsorbed catalyst because the experiments with the highly polished electrode (Figure 2A) showed clearly that [(tim)Co]²⁺ in solution exhibits no catalytic activity at potentials as positive as that of the peak potential of the catalytic current in Figure 5A.

The catalytic reduction of O₂ at a roughened rotating EPG disk electrode is shown in Figure 5B. A well-developed cathodic plateau is obtained which was not the case with highly polished rotating disk electrodes (Figure 2B). Levich²¹ and Koutecky–Levich plots^{22,23} were prepared from current-potential curves like that in Figure 5B by subtracting the plateau current for the reduction of [(tim)Co]³⁺ at the same rotation rate (dotted curve in Figure 5B) from the measured plateau currents. The results, shown in parts C and D of Figure 5, demonstrate that the reduction of O₂ proceeds at close to the diffusion-convection-controlled rate (the y-axis intercept of the line in Figure 5D is small, even in an O₂-saturated solution (inset)) to yield H₂O₂ (the data points in parts C and D of Figures 5 fall close to the calculated lines for the diffusion-convection-limited two-electron reduction of O₂). In accord with these results was the observation that the adsorbed [(tim)Co]^{3+/2+} couple exhibited negligible catalytic activity toward H₂O₂ in the absence of O₂. The intercept of the line drawn through the experimental points in the inset in Figure 5D was used to estimate a second-order rate constant for the formation of the [(tim)CoOO]²⁺_{ads} adduct on the electrode surface.^{23,24} The value obtained was $k_2 \sim 10^5$ M⁻¹ s⁻¹.

Discussion

A catalytic mechanism that is compatible with the behavior observed in Figure 5 is given in reactions 1–4.



(21) Levich, V. G. *Physicochemical Hydrodynamics*; Prentice Hall: Englewood Cliffs, NJ, 1962.

(22) Koutecky, J.; Levich, V. G. *Zh. Fiz. Khim.* **1956**, *32*, 1565.

(23) Oyama, N.; Anson, F. C. *Anal. Chem.* **1980**, *52*, 1192.

(24) Andrieux, C. P.; Savéant, J.-M. *J. Electroanal. Chem.* **1982**, *134*, 163.

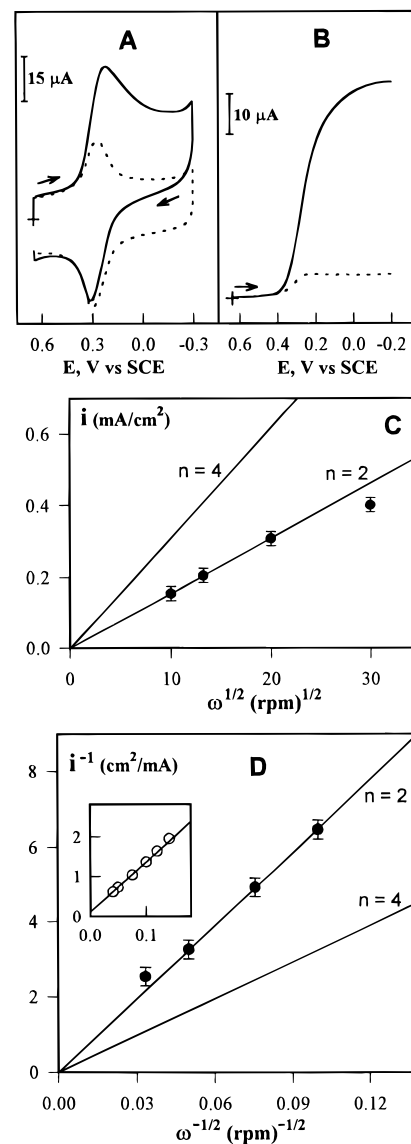
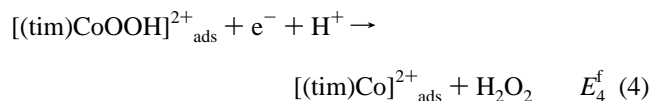
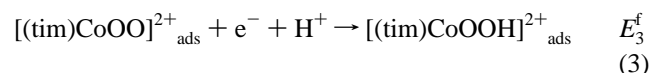
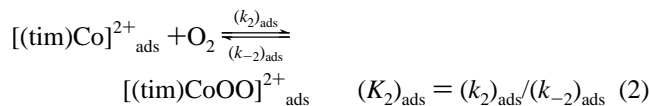


Figure 5. (A) Cyclic voltammograms recorded with a roughly polished EPG electrode (0.32 cm²) in a solution containing 0.1 mM [(tim)Co]³⁺ in the absence of O₂ (dotted curve) and in an air-saturated solution (solid curve). Scan rate: 50 mV s⁻¹. Supporting electrolyte: 0.2 M CF₃COONa–0.2 M CF₃COOH. (B) Rotating-disk voltammetry for the two solutions in part A. Rotation rate: 100 rpm. (C) Levich plot of plateau currents for curves like the one in part B (corrected for the contribution from the dotted curve) vs the electrode (rotation rate)^{1/2}. (D) Koutecky–Levich plot of the reciprocal currents in part C vs (rotation rate)^{-1/2}. The points are experimental; the solid lines are the calculated responses for the diffusion-convection-limited reduction of O₂ by 2 or 4 electrons. The inset shows the currents obtained in an O₂-saturated solution with extrapolation to the origin of the line drawn through the experimental points with the calculated slope for $n = 2$.



Formal potentials E_3^f and E_4^f are unknown but they must be at least as positive as 0.3 V to account for the presence of only

one cathodic peak in Figure 5A where the reduction of $[(\text{tim})\text{Co}]^{3+}$ and the catalyzed reduction of O_2 proceed simultaneously. In the case of the analogous $[(\text{hmc})\text{CoOO}]^{2+}_{\text{ads}}$ and $[(\text{hmc})\text{CoOOH}]^{2+}_{\text{ads}}$ complexes, E_3^f and E_4^f were estimated as 0.64 and 0.12 V (vs SCE at pH 1), respectively.⁶ This value of E_3^f is over 0.5 V more positive than the formal potential of the $[(\text{hmc})\text{Co}]^{3+/2+}_{\text{ads}}$ couple⁶ and a similar positive shift in the formal potentials for the tim complex would not be surprising.

The value of E_4^f for half-reaction 4 must be more positive than the value estimated for the corresponding $[(\text{hmc})\text{CoOOH}]^{2+}_{\text{ads}}$ complex (0.12 V) in order to account for the observed catalytic reduction of O_2 to H_2O_2 in a single voltammetric step near 0.25 V (Figures 5A and 5B). A possible reason why the value of E_4^f might be more positive for the $[(\text{tim})\text{CoOOH}]^{2+}_{\text{ads}}$ than for the $[(\text{hmc})\text{CoOOH}]^{2+}_{\text{ads}}$ complex is offered in the next section.

The equilibrium constant for reaction 2 is also unknown. The equilibrium constant for the same reaction involving reactants in solution has been estimated to be ca. 1 M^{-1} ,¹⁴ but it could be considerably larger for $[(\text{tim})\text{Co}^{2+}]_{\text{ads}}$ if the functional groups present on the surface of the roughened graphite electrode coordinated to an axial position of the Co(II) center of the adsorbed complex to enhance its affinity for O_2 .^{10,13,14}

The density of functional groups on graphite surfaces can also be increased by aggressive electro-oxidation of the surface²⁵ rather than by roughly polishing it. Electrooxidation of the surface proved successful in enhancing the catalytic activity of $[(\text{tim})\text{Co}]^{3+/2+}_{\text{ads}}$ at highly polished EPG electrodes. The response from electrodes like the one in Figure 2B that exhibited limited catalytic activity was converted into one resembling that shown in Figure 5A by oxidation of the surface at 1.8 V for 30 s. in 0.1 M H_2SO_4 followed by reduction at -0.2 V for 15 s. The adsorption of the complex is not as great on the oxidized as it is on the roughened graphite surface, but the enhancement in catalytic activity is comparable. The behavior supports the speculation that functional groups on the surface are important in enhancing the rate of the catalytic reduction by increasing the value of $(K_2)_{\text{ads}}$.

Comparison of the Homogeneous and Heterogeneous Catalytic Reductions of O_2 by $[(\text{tim})\text{Co}]^{2+}$. In homogeneous solutions the $[(\text{tim})\text{Co}]^{2+}$ complex plays the dual roles of coordinative activator of O_2 toward reduction (or stabilizer of the resulting O_2^-) and supplier of electrons to reduce the coordinated O_2 . This process is quite slow, probably because the concentration of coordinated O_2 is very low.¹⁴ When the $[(\text{tim})\text{CoOO}]^{2+}_{\text{ads}}$ adduct is formed on the electrode surface, the electrons for its reduction can be supplied by the electrode at a rate that depends exponentially on the electrode potential and does not require collisions with additional $[(\text{tim})\text{Co}]^{2+}$ complexes. The cross-sectional concentration of $[(\text{tim})\text{Co}]^{2+}$ is much greater on a saturated surface than it is in homogeneous solutions containing a few millimoles per liter of the complex. In addition, as suggested by the results discussed above, the equilibrium constant for reaction 2 may also be greater on the surface than it is in solution. The combination of these two features could account for the higher rate of the catalytic reduction of O_2 at catalyst-coated electrodes than in homogeneous solutions of the catalyst.

The very slow homogeneous reduction of O_2 by $[(\text{tim})\text{Co}]^{2+}$ was found to yield H_2O , and H_2O_2 was ruled out as a (subsequently reduced) intermediate.¹³⁻¹⁵ This stoichiometry contrasts with the quantitative reduction of O_2 to H_2O_2 at

electrodes coated with $[(\text{tim})\text{Co}]^{3+/2+}_{\text{ads}}$. The difference is most simply explained by considering the properties of the cobalt(III) hydroperoxide intermediate, $[(\text{tim})\text{CoOOH}]^{2+}$, thought to be formed in both cases. In solution, the coordinated hydroperoxide can be reduced by an inner-sphere pathway involving a transition state with another $[(\text{tim})\text{Co}]^{2+}$ complex coordinated to an oxygen atom of the hydroperoxide.¹³ In contrast, at the electrode the Co(III) center of the adsorbed hydroperoxide complex is more rapidly reduced than the coordinated hydroperoxide ligand because the latter requires an inner-sphere pathway²⁶ which the electrode surface evidently does not provide. Reduction of the Co(III) center produces a labile complex from which the coordinated O_2H^- ligand is rapidly lost and the reduction of O_2 stops at the H_2O_2 stage. An argument analogous to this one was offered previously⁵ to account for the observation that electroreduction of the structurally similar $[(\text{hmc})\text{CoOOH}]^{2+}$ complex yields $[(\text{hmc})\text{Co}]^{2+}$ and H_2O_2 while chemical reduction by reagents having potential coordination sites for the hydroperoxide ligand that would permit the formation of an inner-sphere transition state yields $[(\text{hmc})\text{Co}]^{3+}$ and H_2O as the reduction products.¹⁵

In contrast with $[(\text{tim})\text{Co}]^{3+}_{\text{ads}}$, the reduction of O_2 at electrodes on which $[(\text{hmc})\text{Co}]^{3+}$ is adsorbed proceeds in two separated steps with $[(\text{hmc})\text{CoOOH}]^{2+}_{\text{ads}}$ produced as an observable intermediate that requires a more negative potential for its reduction (to $[(\text{hmc})\text{Co}]^{2+}_{\text{ads}}$ and H_2O_2) than the potential where the $[(\text{hmc})\text{Co}]^{3+}_{\text{ads}}$ is reduced in the presence of O_2 . With the $[(\text{tim})\text{Co}]^{3+}_{\text{ads}}$ complex no corresponding $[(\text{tim})\text{CoOOH}]^{2+}_{\text{ads}}$ intermediate was detectable, presumably because it is further reduced (to $[(\text{tim})\text{Co}]^{2+}_{\text{ads}}$ and H_2O_2) at the same potential where the reduction of $[(\text{tim})\text{Co}]^{3+}_{\text{ads}}$ occurs in the presence of O_2 . The formal potential for the reduction of the $[(\text{hmc})\text{CoOOH}]^{2+}_{\text{ads}}$ complex was estimated to be 0.12 V at pH 1,⁶ but the results obtained in the present study require a formal potential at least 0.2 V more positive for the $[(\text{tim})\text{CoOOH}]^{2+}_{\text{ads}}$ complex. The much weaker affinity for superoxide anions of the $[(\text{tim})\text{Co}]^{3+}$ complex than of the $[(\text{hmc})\text{Co}]^{3+}$ complex ($K_2 \sim 1$ vs $2.2 \times 10^3 \text{ M}^{-1}$) is likely to extend to the corresponding hydroperoxide complexes on the basis of results and arguments given in ref 5. The less stable $[(\text{tim})\text{CoOOH}]^{2+}_{\text{ads}}$ complex would be expected to exhibit a more positive formal potential, as observed. In addition, the irreversible electroreduction of $[(\text{hmc})\text{CoOOH}]^{2+}$ proceeds at considerably more positive potentials when the complex is adsorbed on graphite where interaction of the Co(III) center with the graphite surface has been speculated to weaken the bond to the O_2H^- ligand and facilitate its reductive breakage.⁶ The $[(\text{tim})\text{CoOOH}]^{2+}_{\text{ads}}$ complex probably interacts with the graphite surface more strongly than the $[(\text{hmc})\text{CoOOH}]^{2+}_{\text{ads}}$ complex because of both the absence of the six methyl groups that interfere with the close approach of the central Co(III) ion to the surface and the presence of the four double bonds in the tim ligand that constrain the macrocyclic ring into flatter configurations. One result could be a greater adsorption-induced weakening of the cobalt(III)-oxygen bond in $[(\text{tim})\text{CoOOH}]^{2+}_{\text{ads}}$ and a correspondingly more positive potential for its reduction to $[(\text{tim})\text{Co}]^{2+}_{\text{ads}}$ and H_2O_2 .

Conclusions

The $[(\text{tim})\text{Co}]^{3+/2+}$ couple serves as a catalyst for the electroreduction of O_2 to H_2O_2 at graphite electrodes only when it is adsorbed on the surface of the electrode. In solution, the binding of O_2 by the complex is too weak to yield significant catalytic reduction currents. The much higher catalytic currents

(25) Cabaniss G. C.; Diamantis, A. A.; Linton, R. W.; Murphy, W. R.; Meyer, T. J. *J. Am. Chem. Soc.* **1985**, *107*, 1845.

(26) See ref 15 and references cited there.

obtained from the adsorbed catalyst are believed to result from an increase in its affinity for O₂ induced by interaction of the Co(II) center with functional groups on the electrode surface. The catalyzed reduction of O₂ to H₂O₂ occurs in a single voltammetric step at a potential, 0.25 V, close to that where [(tim)Co]³⁺_{ads} is reduced to [(tim)Co]²⁺_{ads} in the absence of O₂. This potential is notably more positive than that where the analogous [(hmc)Co]^{3+/2+}_{ads} complex catalyzes the electroreduction of O₂.⁶ The difference in behavior is attributed to the higher reactivity toward electroreduction of the Co(III) center

in [(tim)CoOOH]²⁺_{ads} (presumed to be formed as an undetected intermediate) than in the corresponding [(hmc)CoOOH]²⁺_{ads} complex, which is more stable.⁵

Acknowledgment. This work was supported by the National Science Foundation. I.B. was the grateful recipient of an A. A. Noyes Postdoctoral Fellowship at Caltech. Discussions with Dr. Beat Steiger were stimulating and very helpful.

IC9608399